CORA Cork Open Research Archive
Cartlann Taighde Oscailte Chorcaí

Title	Automated baseline correction evaluation score for Raman spectroscopy
Authors	Innocente, Simone;Visentin, A.;Andersson-Engels, S.;Komolibus, K.;Gautam, R.
Publication date	2026-04-23
Original Citation	Innocente, S, Visentin, A, Andersson-Engels, S, Komolibus, K & Gautam, R 2026, 'Automated baseline correction evaluation score for Raman spectroscopy', ACS Omega, vol. 11, no. 17, pp. 25057-25068. https://doi.org/10.1021/acsomega.5c09870
Type of publication	Article (peer-reviewed)
Link to publisher's version	https://www.scopus.com/pages/publications/105037855058 - 10.1021/acsomega.5c09870https://www.scopus.com/pages/publications/105037855058?origin=resultslist
Rights	Publisher Copyright: © 2026 The Authors. Published by American Chemical Society. - https://creativecommons.org/licenses/by-nc-nd/4.0/
Download date	2026-11-14 16:31:57
Item downloaded from	https://hdl.handle.net/10468/18751


UCC
University College Cork, Ireland
Coláiste na hOllscoile Corcaigh

ACS OMEGA

Open Access

This article is licensed under CC-BY-NC-ND 4.0

http://pubs.acs.org/journal/acsodf

Article

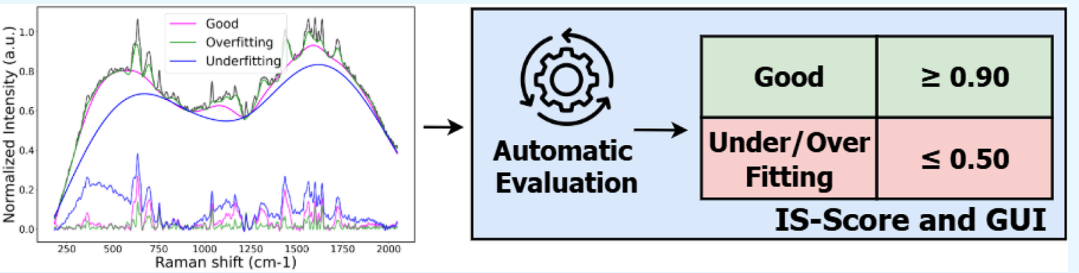
Automated Baseline Correction Evaluation Score for Raman Spectroscopy

Simone Innocente,* Andrea Visentin, Stefan Andersson-Engels, Katarzyna Komolibus, and Rekha Gautam*

Cite This: *ACS Omega* 2026, 11, 25057−25068

Read Online

ACCESS | Metrics & More | Article Recommendations | Supporting Information



ABSTRACT: Raman spectroscopy is a noninvasive technique providing detailed molecular insights into tissue composition, enabling applications in diagnostics and therapy monitoring. However, Raman signals are inherently weak and prone to superimposed background signals, making baseline correction, a critical step to remove background signals, essential. Typically, experts assess the quality of baseline fitting visually, which is subjective, time-consuming, and impractical with large clinical data sets. To address this, we propose the IS (Integrity Spectrum) Score, a quantitative and automatic metric that evaluates baseline correction quality directly from Raman spectra. The algorithm leverages several spectral properties: it measures the distance between the baseline and the band's prominence, quantifies the Raman shift distances within band edges using a band prominence−proportional factor, compares area-under-the-curve differences between the raw spectrum and an intentionally overfitted baseline, and counts dips where the baseline rises above the spectral curve. These combined indicators capture both underfitting and overfitting behaviors without requiring ground truth labels or manual inspection. Results obtained using complex two-layered blood cell data sets show a strong correlation between IS-Score and expert evaluations, while substantially reducing the time required from experts. This method supports multicenter studies by facilitating consistent baseline correction, reducing labor, and minimizing subjective bias, ultimately enhancing the reliability and comparability of Raman data for clinical research.

Downloaded via 212.129.74.158 on May 12, 2026 at 10:10:28 (UTC).
See https://pubs.acs.org/sharingguidelines for options on how to legitimately share published articles.

INTRODUCTION

Raman spectroscopy is based on inelastic scattering of light, noninvasively providing insights about molecular structures and interactions in various samples.[1] The Raman signal is inherently weak, which makes the data highly susceptible to any background signal as well as noise. The typically weak signals underscore the importance of careful data preprocessing to minimize interferences from background signals and calibration errors.[2] Failure to address these issues adequately can negatively impact the results of subsequent qualitative or quantitative analysis.[3] In the preprocessing step of Raman spectra, baseline correction plays a crucial role in eliminating unwanted background signals such as fluorescence. Over the years, various approaches have been developed to improve the baseline computation for Raman spectra, such as polynomial fitting,[4,5] and penalized least-squares-based methods,[6] to more advanced techniques involving wavelet transforms,[7,8] morphological operations-based,[9] and machine learning.[10−12] However, choosing an algorithm is not straightforward. Figure 1A illustrates a classic baseline algorithm selection workflow. In

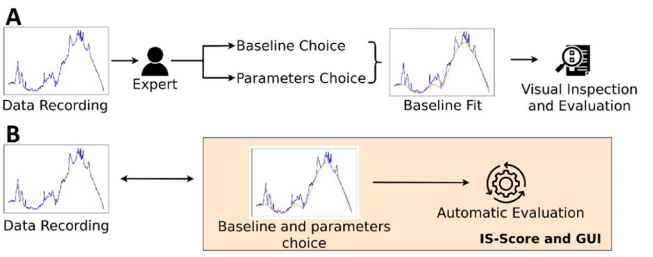


Figure 1. (A) Classic approach to baseline correction algorithm choice. (B) New approach with the IS-Score.

Received: September 22, 2025
Revised: January 18, 2026
Accepted: January 26, 2026
Published: April 23, 2026



© 2026 The Authors. Published by American Chemical Society

this approach, the quality of a baseline is typically assessed by an expert through visual inspection to determine whether it adequately fits a given Raman spectrum. This step is crucial as an inadequately fitted baseline may inadvertently alter the shape and amplitude of important chemical bands in the Raman spectra, potentially leading to the loss of critical information or the introduction of additional peaks not corresponding to biological features. To evaluate the effectiveness of a baseline correction algorithm, the standard approach involves comparing it with a baseline fitted by an expert using metrics such as Root Mean Squared Error (RMSE).

He et al[13] computed the RMSE for each of the many methods proposed and manually examined regions of the spectra where the background was not well fitted, where error is defined as the difference between the true baseline from simulated data and the estimated baseline. Liu et al.[14] defined the AC_rate to quantify the accuracy of the fitting results, where AC_rate measures how closely the estimated baseline matches the true baseline. Despite its utility, it still depends on a ground truth baseline to perform a comparison between the fitted baselines. Similarly, Sheehy et al.[15] generated benchmark spectra by combining Raman and baseline components, providing a Raman target against which baseline-corrected spectra could be evaluated using the normalized mean squared error (nMSE). However, relying solely on synthetic data is inadequate, given the diversity of domains where Raman spectroscopy is applied. Recently, Ou et. al[16] proposed a method to assess baseline correction by evaluating the correlation of Raman spectral parameters measured at two excitation wavelengths. A positive correlation is expected if the baseline is accurately removed. Although this approach provides a data-driven way to evaluate the baseline correction, it requires measurements at multiple wavelengths, limiting its applicability. Guo et al. calculated a numerical quantitative marker to evaluate baseline quality which was also integrated with a genetic algorithm to automatically estimate the optimal baseline, though validation was limited to averaged spectra.[17] When dealing with multiple spectra from the same sample, the process of assessing the baseline for each individual spectrum becomes highly labor-intensive, time-consuming, and prone to errors. To manage this complexity, the expert selects a small subset of spectra representing different classes from the data set and visually inspects various baseline correction algorithms and their associated parameters with the goal of identifying a baseline method that adequately fits the selected subset. Once a suitable algorithm is found, it is applied to the entire data set, assuming that it will perform equally well on all the spectra. However, this methodology has significant limitations as it relies heavily on the assumption that the subset of spectra chosen for evaluation is representative enough of the entire data set. In practice, this may not always be the case, as Raman spectra from the same sample can exhibit variability due to factors such as instrumental noise, sample heterogeneity, and environmental conditions. If the subset does not capture this variability, the chosen baseline correction algorithm may not generalize well to the entire data set. This can lead to suboptimal baseline corrections for spectra that differ from those in the subset, potentially distorting important chemical information or introducing artifacts and a lack of reproducibility. An additional limitation lies in the manual selection of baseline algorithms and parameters, which is inherently subjective and dependent on the expertise of the individual performing the evaluation. Different experts might choose different baselines for the same subset of spectra, leading to inconsistencies in the preprocessing pipeline. This subjectivity, combined with the potential lack of representativeness in the subset, underscores the need for a more robust, automated, and objective approach to baseline evaluation.

This paper introduces a quantitative metric called **IS (Integrity Spectrum) Score** to assess baseline fit quality, starting from a Raman spectrum and a baseline-corrected version of the spectrum. This approach does not rely on ground truth values or domain-expert visual inspections but instead uses a mathematical formulation that captures the key aspects that experts typically consider when evaluating baseline quality. The metric leverages various properties of a Raman spectrum such as peak positions, intensity values, and area under the curve (AUC). It is an automatic methodology and not only reduces the labor-intensive nature of the process but also ensures that the baseline correction algorithm performs consistently across a set of spectra, regardless of their variability. Figure 1B presents the proposed workflow incorporating the IS-Score in a computer app, where an expert can choose a baseline correction algorithm and parameters to test, and an automatic evaluation is performed across a single spectrum or an entire folder. This app combines an automated baseline evaluation process with a custom-designed graphical user interface (GUI) to enhance usability. The IS-Score ranges from 0 to 1, where a value close to 1 indicates a better fit and a value close to 0 indicates poor fitting.

Raman spectroscopy is widely used across diverse fields such as material science, chemical analysis, medical diagnostics, and food science,[18−20] owing to its ability to provide molecular insight into samples. However, the wide variety of spectra of interest becomes a challenge when designing a generic data preprocessing tool. Indeed, each spectrum can vary in intensity, frequency range, background shape, and peak position due to instrumental settings, environmental conditions, or sample heterogeneity. The algorithm needs to be as generic as possible and take all of these variables into consideration. Moreover, the subjective nature of this task complicates the establishment of a universally accepted definition of what constitutes a *good* baseline. Different experts may have varying opinions on the performance of the same baseline correction algorithm depending on their specific experience or application domain. This subjectivity arises because the choice of a good baseline is not only a technical task but also involves a degree of interpretation and judgment. The IS-Score was developed to provide a generic and objective evaluation of the baseline correction performance across diverse spectra. Furthermore, to facilitate wider adoption, we provide a Python package with a user-friendly GUI for streamlined evaluation.

METHODOLOGY

Raman Data Set

To assess the performance and robustness of the IS-Score, two experiments were conducted using distinct Raman spectroscopy data sets published previously.[21] Briefly, Raman data were acquired using a Renishaw Invia microspectrometer (Renishaw Inc., West Dundee, IL) equipped with a 633 nm laser and using a 5× (NA = 0.12) objective. The first experiment comprises diffuse resonance Raman spectra from isolated red blood cells and polymer bags,[21] including 150 spectra within

https://doi.org/10.1021/acsomega.5c09870
ACS Omega 2026, 11, 25057−25068

Table 1. Overview of the Penalization Methods with Evaluation and the Underlying Idea for Each Block Available in the Algorithm

Penalization	Evaluation	Idea
Single Band (Peak & Dip)	Measure the distance between baseline and band prominence.	Prominence evaluation helps detect overfitting or underfitting of the baseline.
Band Region (Peak & Dip)	Evaluate Raman shifts between the edges using a value proportional to the band prominence.	Extend the single band concept to a wider region to assess baseline fitting. $\mathrm{BandRegion}_{\mathrm{Penalization}} = \mathrm{Penalty}_{\mathrm{Overfitting}} + \mathrm{Penalty}_{\mathrm{Underfitting}}$
AUC	Compare raw-spectrum AUC with an overfitting baseline AUC.	An overfitting baseline's AUC should closely match the uncorrected spectrum AUC. $\mathrm{AUC}_{\mathrm{Penalization}} = \mathrm{Initial}_{\mathrm{Penalty}} + \mathrm{Addon}_{\mathrm{Penalty}}$ where $\mathrm{Initial}_{\mathrm{penalty}} = \frac{\mathrm{AUC}_{\mathrm{baseline\ corrected\ spectrum}}}{\mathrm{AUC_raw\ spectrum}} \pm \frac{\mathrm{AUC}_{\mathrm{overfitted\ baseline\ corrected\ spectrum}}}{\mathrm{AUC_raw\ spectrum}}$ $\mathrm{Addon}_{\mathrm{Penalty}} = \frac{\mathrm{AUC}_{\mathrm{Negative}} \text{ or } \mathrm{AUC}_{\mathrm{positive}}}{\mathrm{AUC}(\mathrm{Baseline}_{\mathrm{Corrected}})}$
Mean Ratio	Count the dips that are above and below the baseline.	A realistic baseline allows some spectral dips to remain below it, if too few, it is likely underfitting. $\mathrm{MeanRatio}_{\mathrm{Penalization}} = \sum_{\mathrm{Sp}}^{\mathrm{Sp}_{\mathrm{Denoised}}} \left(\frac{1}{n} \sum_{i}^{\mathrm{Dips}_{\mathrm{Greater}}} \mathrm{Baseline}_i - \mathrm{SpDenoised}_i \right)$
Intensity	Count the number of Raman shifts where the baseline exceeds the spectrum.	A correct baseline should stay below most of the spectrum to preserve real spectral features. $\mathrm{Intensity}_{\mathrm{Penalization}} = \frac{\#\mathrm{Penalized}_{\mathrm{RS}}}{(\#\mathrm{Total}_{\mathrm{RS}} - \#\mathrm{Penalized}_{\mathrm{RS}})}$

the Raman shift range of 182−2046 cm^{-1}. In this case, an Asymmetric Least Squares (ASLS) baseline correction algorithm was applied with three configurations: the penalizing weighting factor p was fixed at 0.007, while the smoothing parameter λ was varied across 100, 2×10^3, and 2×10^4 to examine the effect of different regularization strengths. The second experiment contains more complex two-layer diffuse resonance Raman spectra from red blood cells stored in polymer bags.[21] While the first data set involved spectra acquired from isolated materials, this data set represented a two-layer configuration where blood signals were measured through the polymer layer. Here, both blood and polymer backgrounds influence the baseline shape, making correction more challenging. This data set also includes 150 spectra within the same Raman shift range (182−2046 cm^{-1}). For this case, three different baseline correction algorithms were evaluated: ASLS (λ = 2000, p = 0.005), BubbleFill (minimum bubble width = 100), and Modified Polynomial (ModPoly, 10th order).

Computation

All analyses and the algorithm were performed using Python 3.11. Numerical computations were performed with NumPy, while interpolation and signal processing routines were implemented using SciPy. For robust detection and analysis of peaks and valleys, the findpeaks[22] library was also exploited.

Approach

In this section, a general overview of the baseline evaluation algorithm is provided (Table 1). A particular focus is to address *underfitting* (to avoid artifact peaks) and *overfitting* (to avoid loss of features) of the baseline. Figure 2 shows an example of these phenomena alongside the baseline-corrected version of the spectra. An underfitting baseline (blue) correction fails to properly capture the fluorescence background, leading to insufficient correction. Conversely, an overfitting baseline (green) adheres too closely to the spectral

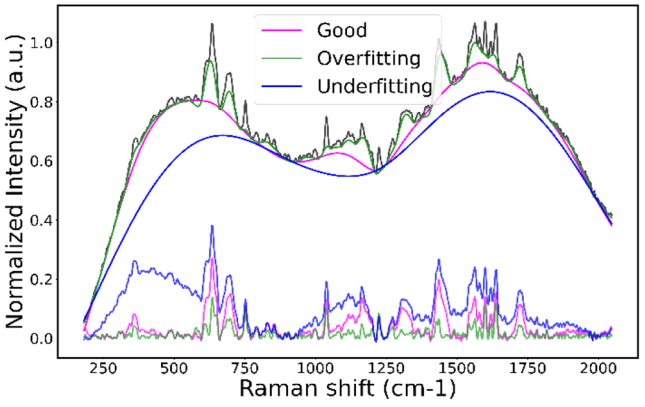


Figure 2. Examples of overfitting (green), underfitting (blue), and good (magenta) baselines and the resulting corrected spectra.

signal, potentially removing or distorting important Raman peaks. The baseline-corrected spectra presented in Figure 2 were produced using static baseline correction with predefined parameters and were not optimized dynamically by using the IS-Score. These baselines were specifically selected to illustrate representative cases of overfitting and underfitting, motivating the need for the proposed IS-Score metric. A high-level overview of the IS-Score algorithm is provided in Figure 3.

The algorithm requires three inputs: the raw Raman spectrum, the baseline-corrected spectrum—where background fluorescence has been removed—and the corresponding spectral axis. The output generated is a value that indicates the quality of the baseline correction. It is structured into distinct blocks, each evaluating a specific feature of the fit of the Raman spectrum and the chosen baseline, generating a numerical penalty score based on its assessment. The algorithm incorporates two additional components: a band and an edge detection algorithm. The first is used to identify the most significant peaks and dips within a Raman spectrum,

https://doi.org/10.1021/acsomega.5c09870
ACS Omega 2026, 11, 25057−25068

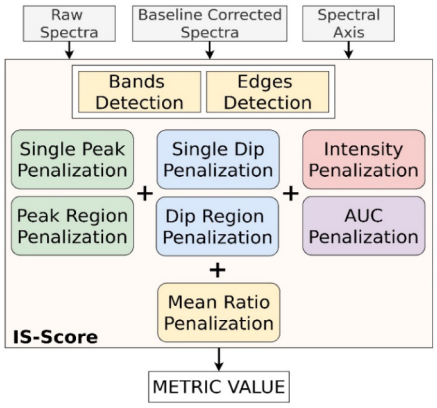


Figure 3. General overview of the IS-Score computation with different penalization blocks.

while the second determines the edges (local minima) associated with each specific band. Together these algorithms provide information about the spectral features, enabling a more precise evaluation of the baseline and its alignment with the Raman signal.

Let $I(\tilde{\nu}) = [I(\tilde{\nu}_1), I(\tilde{\nu}_2), \ldots, I(\tilde{\nu}_z)]$ and $B(\tilde{\nu}) = [B(\tilde{\nu}_1), B(\tilde{\nu}_2), \ldots, B(\tilde{\nu}_z)]$ denote, respectively, the measured Raman intensity and the estimated baseline evaluated over the same discrete set of wavenumbers $\{\tilde{\nu}_1, \tilde{\nu}_2, \ldots, \tilde{\nu}_z\}$. The penalties from each block are added, retrieving the total penalty (1).

$$\text{Total}_{\text{Penalization}} = \sum_{i}^{n_{\text{blocks}}} \text{block}_i(I(\tilde{\nu}), B(\tilde{\nu})) \quad (1)$$

Finally, the IS-Score is computed by subtracting the total penalties from 1. Table 1 showcases the evaluation and the idea behind each penalization block.

Construction of the Algorithm Parameters

One of the challenges mentioned above lies in the Raman spectra variability, both in intensity and frequency range. To ensure a fair comparison across different baseline correction algorithms applied to the same spectrum, normalization is required. Two distinct normalization strategies were performed, each serving a specific purpose:

Spectrum-Only Normalization: This normalization scales the raw Raman spectrum to the [0, 1] range based on its own minimum and maximum values. It is used for band and region detection, which depends on the shape of the signal, independent of any baseline. This ensures that feature detection is consistent and not biased by any particular baseline correction method.

Joint Spectrum-Baseline Normalization: When evaluating how well a baseline correction method performs, both the original spectrum and its baseline are normalized together using the global minimum and maximum across both signals. This ensures that comparisons are meaningful and not distorted by mismatched scaling.

Using two normalizations allows us to divide the process of feature detection and baseline evaluation, ensuring consistent detection across spectra and fair evaluation of baseline corrections, and preserving the structural integrity and comparability of the signals.

During testing, multiple threshold and parameter values were evaluated on different representative spectral data sets, and their impact on the IS-Score sensitivity and robustness was assessed. These thresholds were chosen based on their ability to produce stable IS-Score values across the test data set, reflecting consistent feature detection without oversensitivity to minor fluctuations. A comprehensive parameter sensitivity analysis, including the influence of peak prominence thresholds and the logarithmic term coefficient on the IS-Score stability is provided in the Supporting Information (Figures S6 to S30).

Bands and Edges Detection

Positive bands (peaks) are key features of a Raman spectrum, revealing important insights into the chemical composition and structure of the sample. The IS-Score algorithm provides an automated band detection process that identifies the main peaks as well as dips, which are defined as positive bands in the inverted signal. The algorithm operates by finding bands that consistently appear in both the raw and denoised versions of the spectrum. It compares two sets of bands, one from the raw spectrum and one from the denoised spectrum, and considers a specific band to be *common* if:

- it is present in the raw spectrum, and
- its position differs by no more than five Raman shift units (cm^{-1}) from the position of a band in the denoised spectrum.

To ensure that the band detection is reliable and robust to noise, the method analyzes multiple smoothed versions of the spectrum. Only bands that appear in at least two denoised iterations are retained, highlighting the most robust and meaningful features. Figure 4 shows a simplified illustration of

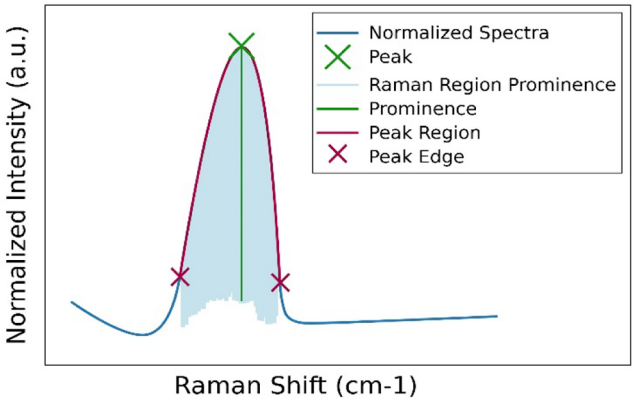


Figure 4. Peaks (green cross), peak region (purple), peak edges (purple cross), prominence (green line), and Raman Region Prominence (light blue area) detected by the band and edge detection blocks.

the band and edge detection mechanism. Each band is detected based on its *prominence* that indicates how much a band stands out compared to the surrounding signal, ensuring that only the most significant bands in the Raman spectrum are selected. The prominence of each spectral band was calculated using the *peak_prominence* function available in the SciPy library.[23] For each detected peak, prominence is defined as the vertical distance between the peak intensity and the higher of its two surrounding minima. This method accounts for adjacent peak interference by determining minima within the intervals bounded by the signal's ascent to higher peaks. Edges are defined as Raman shift values where the band begins to rise

https://doi.org/10.1021/acsomega.5c09870
ACS Omega 2026, 11, 25057−25068

(left edge), reaches its peak, and then decreases to its lowest point (right edge) (Figure 4). The algorithm locates a relative minimum of a denoised version of the spectrum to set the initial left or right edge for each band. Subsequently, it searches for the nearest points in the original spectrum where the intensity closely matches those of the selected edges, thereby approximating the edges for each band. To further strengthen the results, the detected edges are refined with those obtained from an alternative peak-detection method.[22] This is done by comparing the distances from each band to its left and right edges in both methods, ensuring that the band boundaries are consistent and reliable. This combined approach improves the accuracy of the edge determination, contributing to a more reliable spectral analysis. The process is repeated for all bands identified during the initial detection.

Single Peak and Dip Penalization

The first penalization aims to mitigate baseline overfitting and underfitting by leveraging band prominence analysis. After the bands and their edges within the spectrum are identified, the prominence for each band is calculated. Peaks are exploited to assess potential overfitting by defining an *evaluation point*, located by subtracting 75% of the peak's prominence from its intensity value. This point serves as a critical boundary: if the baseline intensity at the peak's position (Raman shift location) exceeds this threshold, the peak is flagged for penalization. For robustness, a secondary check is implemented using a stricter evaluation point, calculated using the 75% prominence, with an additional value corresponding to half of the distance between the baseline intensity value and the original prominence. This two-step examination approach improves sensitivity and helps identify more subtle instances of overfitting. Underfitting is assessed through dips evaluation by defining two different *evaluation points*. Specifically, the block checks whether the baseline lies above the first evaluation point—defined as *half the dip's prominence*—or *below* the second evaluation point corresponding to the *full dip prominence*. The specific cutoffs (75% and half of the distance for peaks, 50% and 100% for dips) were selected as thresholds after empirical testing on diverse spectra.

The idea is that a well-fitted baseline should closely follow the dips in the spectrum. In contrast, an underfitted baseline tends to deviate from these features. Once the set of penalized bands is identified, the penalization is computed through several steps to ensure a controlled and adaptive effect. Initially, the ratio between the penalized peaks and the total number of peaks is calculated. This ratio is used to derive a weighting factor that scales the penalty based on the proportion of affected peaks. To prevent excessive penalization when many peaks are flagged, a scaling factor, beta, is introduced. Let N denote the total number of bands and M the number of penalized bands. The ratio is defined in eq 2 and the scaling factor in eq 3.

$$\text{ratio} = \frac{M}{N} \tag{2}$$

$$\beta = \max(1, \mathrm{N} \times (1\text{-ratio})) \tag{3}$$

This ensures that the penalization remains moderate, even when the ratio is high. Further, a weight (eq 4) is defined to balance the impact of penalization relative to the number of bands.

$$w = \frac{\sqrt{\mathrm{N}}}{\sqrt{\mathrm{N}} + \beta} \tag{4}$$

This formulation ensures the penalty increases more gradually for a smaller number of penalized bands, avoiding overpenalization when few bands are flagged. To further refine the penalization, a logarithmic term is introduced to provide a smooth, nonlinear increase in the penalty value (eq 5). The value 1.5 was chosen arbitrarily, as the algorithm was developed through an iterative process aimed at aligning as closely as possible with expert judgment.

$$\log_{\text{term}} = \log(1.5 + \text{ratio}^2) \tag{5}$$

Finally, the overall penalization is computed as the product of the weight w and the logarithmic term as shown in eq 6

$$\text{SingleBand}_{\text{Penalization}} = w \times \log_{\text{term}} \tag{6}$$

This formulation ensures an adaptive and balanced penalization, preventing extreme penalties while maintaining sensitivity to the proportion of the penalized bands.

Peak and Dip Region Penalization

A similar approach to single-band penalization can be extended to the entire band region. However, prominences are traditionally defined only at the peak location and not across other Raman shift values within the region. Thus, the concept of *Raman Region Prominence (RRP)*, a measure that uses the fitted baseline to estimate a proportional value of prominence at each Raman shift within the band region, is introduced. This allows for a more continuous and informative assessment of the band's significance beyond just the peak location. However, true prominence is defined only for actual peaks (local maxima). To extend prominence estimation beyond the peak, the difference between the signal intensity and the baseline intensity is used to define a pseudoprominence for every Raman shift. For any peak with intensity-to-baseline distance x and actual prominence y, any Raman shift with distance z from the baseline can be assigned a proportionally scaled prominence $p(z)$, enabling a continuous prominence field across the region. The RRP is robust to typical experimental noise levels because peak and edge detection rely on smoothed spectral profiles rather than individual point fluctuations. High-frequency noise minimally affects the intensity-to-baseline distance, and the band-defining edges further reduce sensitivity to spurious fluctuations.

Recalling the previous definitions, $I(\tilde{\nu})$ represents the Raman spectrum, while $\mathrm{B}(\tilde{\nu})$ denotes the baseline spectrum, the distance between the band intensity and the baseline intensity at the band position is computed (eq 7). This quantity is essential for computing the RRP, as it serves as a step toward obtaining a value proportional to the real prominence of the peak under evaluation.

$$\delta_{\text{peak}} = I(\tilde{\nu}_{\text{peak}}) - B(\tilde{\nu}_{\text{peak}}) \tag{7}$$

Let R_p denotes the wavenumber interval corresponding to the pth spectral peak, defined by the left and right edges of the band within the Raman spectrum $I(\nu)$.

$$R_p = [\tilde{\nu}_{p,\text{left}}, \tilde{\nu}_{p,\text{right}}] \tag{8}$$

The difference between each Raman Shift and the baseline intensities in the band region is computed (eq 9).

$$\Delta_{\text{Region}} = |\mathrm{I}(R_p) - \mathrm{B}(R_p)| \tag{9}$$

https://doi.org/10.1021/acsomega.5c09870
ACS Omega 2026, 11, 25057−25068

Then the RRP is calculated using eq 10 and 11 exploiting the prominence ρ at the band position.

$$\frac{\rho_{peak}}{\delta_{peak}} = \frac{RRP}{\Delta_{Region}} \tag{10}$$

$$RRP = \frac{\Delta_{Region} \times \rho_{peak}}{\delta_{peak}} \tag{11}$$

This approach enables region-based penalization, similar to a single-band penalization strategy. To compute the region penalization, the absolute distance between the RRP and the baseline is obtained (eq 12).

$$RRP_{Dist} = |RRP - B(R_p)| \tag{12}$$

These distances (eq 12) are used as the basis for overfitting and underfitting penalization because a well-fitted baseline should accurately reflect not only the peak itself but also the surrounding region in which the peak is defined. To optimize the impact on the final calculation, the 75th percentile of the calculated distances is used as a threshold. Only distances below this threshold are retained, and their means are computed to generate two penalty values. Let $Over_{RS}$ denote the number of Raman Shifts (region) where the RRP_{Dist} is lower than the baseline intensity$B(R_P)$, and $Under_{RS}$ denotes those where the distance exceeds the baseline intensity. The overfitting penalty is defined in eq 13 and the underfitting penalty is defined in eq 14 for each individual peak.

$$Overfitting_P = \frac{1}{Over_{RS}} \times \sum RRP_{Dist} \quad \text{if } RRP_{Dist} < Baseline_{Intensity} \tag{13}$$

$$Underfitting_P = \frac{1}{Under_{RS}} \times \sum RRP_{Dist} \quad \text{if } RRP_{Dist} > Baseline_{Intensity} \tag{14}$$

In the case of a dip region, percentile filtering is not applied, as the penalization inherently reflects the presence of underfitting; thus, it needs to be penalized. The total penalization is then obtained by summing all overfitting and underfitting penalties (eq 15) for each band region, resulting in a balanced and region-aware evaluation of baseline quality.

$$BandRegion_{Penalization} = Overfitting_P + Underfitting_P \tag{15}$$

AUC Penalization

This penalty leverages the area under the curve to provide a global assessment of the baseline overfitting. A key challenge in this approach is the lack of a universal AUC reference that defines a well-fitted baseline since spectra can vary significantly in intensity and shape. As a result, simply comparing the AUC of a baseline-corrected spectrum to that of the raw spectrum is not sufficient for a reliable evaluation. To address this, an artificial baseline designed to mimic the overfitting behavior is used, serving as a reference for penalization. This process involves two main steps: the generation of an artificial baseline and the evaluation of the baseline under assessment. The artificial baseline is generated through a multistep procedure that begins with the raw Raman spectrum. First, band regions are replaced using linear interpolation between their respective start and end points, creating a modified signal. The iterative Savitzky−Golay smoothing used in the AUC penalty is physically motivated by the structure of the Raman spectra, where sharp vibrational peaks coexist with slowly varying (low frequency) backgrounds. By progressively increasing the smoothing window size (from 5 to 30, in steps of 5) while maintaining a fixed polynomial order 4, the method sequentially removes high-frequency noise and broader fluctuations across multiple spatial scales in a manner that preserves relevant Raman features. At each smoothing step, spectral dips are identified and a cubic interpolation is fitted through these points. To ensure the resulting baseline remains meaningful, any interpolated value exceeding the corresponding original spectrum point is replaced with the original value, ensuring the interpolation lies below or equal to the spectrum. This process is repeated across six different smoothing levels, producing six distinct interpolation baselines that are averaged to form a robust composite. To further simulate overfitting, a Gaussian-shaped offset was added to the spectral regions corresponding to the detected peaks. The amplitude of each offset was scaled proportionally to 3% of the total intensity range of the spectrum and adjusted proportionally to the individual peak width, ensuring that broader peaks received wider perturbation. Additionally, for spectral regions where the interpolation matches the original intensity, the value is reduced by 0.5% of the difference between the maximum and minimum intensities of the spectrum to avoid exact overlap. Finally, an additional Savitzky−Golay smoothing is applied to obtain the final artificial overfitting baseline. Let $I_B(\tilde{\nu}) = [I_B(\tilde{\nu}_1), I_B(\tilde{\nu}_2), ..., I_B(\tilde{\nu}_z)]$ be the baseline-corrected spectrum, $A(\tilde{\nu}) = [A(\tilde{\nu}_1), A(\tilde{\nu}_2), ..., A(\tilde{\nu}_z)]$ the artificial baseline generated, and $I_A(\tilde{\nu}) = [I_A(\tilde{\nu}_1), I_A(\tilde{\nu}_2), ..., I_A(\tilde{\nu}_z)$ the corrected spectrum with the artificial baseline generated. To calculate the penalty score, two ratios are defined:

- $$BC_{Raman} = \frac{AUC(I_B(\tilde{\nu}))}{AUC(I(\tilde{\nu}))}$$
- $$IC_{Raman} = \frac{AUC(I_A(\tilde{\nu}))}{AUC(I(\tilde{\nu}))}$$

Additionally, the difference between the artificial baseline and the baseline under evaluation (green line in Figure 5) is computed (eq 16).

$$D_{AB}(\tilde{\nu}) = A(\tilde{\nu}) - B(\tilde{\nu}) \tag{16}$$

An initial penalty is defined as the absolute difference between the two ratios.

$$Initial_{Penalty} = |BC_{Raman} - IC_{Raman}| \quad \text{if } AUC(I_B(\tilde{\nu})) > 0 \text{ and } AUC(D_{AB}(\tilde{\nu})) > 0 \tag{17}$$

If either the AUC of the baseline-corrected spectrum or the AUC of their difference is negative, the initial penalization is replaced with the sum of the ratios.

$$Initial_{Penalty} = BC_{Raman} + IC_{Raman} \tag{18}$$

In a second evaluation step, the algorithm analyzes the difference between the artificial and evaluated baselines by

https://doi.org/10.1021/acsomega.5c09870
ACS Omega 2026, 11, 25057−25068

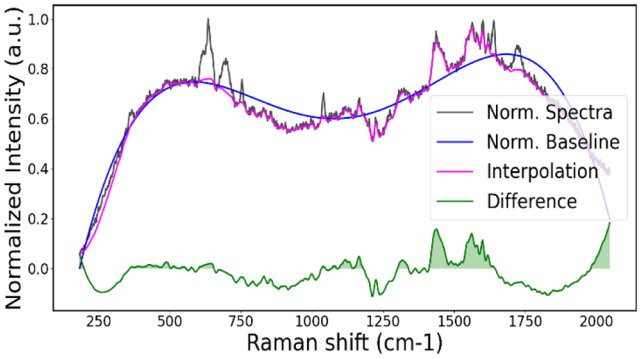


Figure 5. Example of artificial baseline that mimics overfitting baseline (magenta), baseline (blue), and difference between interpolation and baseline (green).

decomposing them into its positive and negative components and computes their respective AUCs.

To further refine the penalization, an addon penalty is introduced based on the relative dominance of the negative or positive AUC. Specifically:

When the total AUC of the difference is negative, or when the negative-to-positive AUC ratio exceeds 0.5, the addon penalty is defined as

$$\text{Addon}_{\text{Penalty}} = \frac{\text{AUC}_{\text{Negative}}}{\text{AUC}(I_{\text{B}}(\tilde{\nu}))} \tag{19}$$

Conversely, when the total AUC is positive and the negative-to-positive AUC ratio is below 0.5, the addon penalty becomes

$$\text{Addon}_{\text{Penalty}} = \frac{\text{AUC}_{\text{Positive}}}{\text{AUC}(I_{\text{B}}(\tilde{\nu}))} \tag{20}$$

The threshold 0.5 was chosen to detect overfitting, as the negative-to-positive AUC ratio greater than 0.5 suggests that more than half of the evaluated baseline lies above the artificial baseline; thus, it is overfitting compared to the artificial baseline. This strategy ensures stronger penalties for overfitting scenarios: since these tend to reduce the AUC of the corrected spectrum, i.e., the denominator of eqs 16 and 17. The final penalization is the sum of the initial and addon penalties.

$$\text{AUC}_{\text{Penalization}} = \text{Initial}_{\text{Penalty}} + \text{Addon}_{\text{Penalty}} \tag{21}$$

Mean Ratio Penalization

This penalization evaluates the baseline fit globally by analyzing the position of spectral dips relative to the baseline. The core principle is that a well-fitted baseline should lie below most of the dips. To ensure robustness, this assumption is evaluated across multiple denoised versions of the spectrum. The process begins with applying a Savitzky−Golay filter to the raw spectrum to generate a smoothed version, from which dips are identified. These dips are then compared to the baseline under evaluation, and the proportion of dips above versus below the baseline is calculated. This procedure is repeated four times with progressively more aggressive smoothing, reducing noise, and stabilizing dip detection. Similar to the AUC penalty, the SG filtering applied here uses a constant polynomial order of 4, while the window length is adjusted to 8, 16, 32, and 40. This configuration was selected to enhance the detection of broader spectral dips as opposed to the narrower features typically associated with peaks. This penalization is applied only when the average ratio across all iterations falls below 50%, indicating that at least half of the dips consistently lie above the baseline, signaling a tendency toward underfitting.

Let $I_{d_i}(\tilde{\nu}) = [I_{d_i}(\tilde{\nu}_1), I_{d_i}(\tilde{\nu}_2), ..., I_{d_i}(\tilde{\nu}_z)]$ be the denoised spectrum at the ith iteration. For each of them, the mean of the distances of all of the dips that exceed the baseline is computed as visible in eq 22, where j corresponds to a specific iteration.

$$\text{Mean}_{\text{Distance}_j} = \frac{1}{n} \sum_{i}^{\text{Dips}_{\text{Greater}}} B(\tilde{\nu}_i) - I_{d_j}(\tilde{\nu}_i) \tag{22}$$

Finally, the mean ratio penalization is the sum of all of the mean distances for each denoised spectrum (eq 23).

$$\text{MeanRatio}_{\text{Penalization}} = \sum_{j}^{I_d(\tilde{\nu})} \text{Mean}_{\text{Distance}_j} \tag{23}$$

Intensity Penalization

This strategy adopts a global perspective, emphasizing that an optimal baseline should follow the underlying trend of the Raman signal without excessive distortion of its features. A well-fitted baseline should rarely, if ever, exhibit intensity values exceeding those of the raw (original) spectrum. Therefore, Raman shift positions where the baseline intensity surpasses the spectral intensity are subject to penalization. However, noise is not relevant to this penalization. To prevent this, a distance-based filtering mechanism is introduced, in which only cases where the baseline exceeds the spectrum by more than a noise-dependent threshold are penalized. This avoids penalizing minor discrepancies that are likely attributable to noise. In order to estimate noise levels, the band regions are exploited and a modified signal is generated by replacing each band region with the corresponding baseline values. This modified signal is smoothed, and the residual—defined as the difference between the original and smoothed signals—is computed. Since spectral peaks and dips are removed, the residual primarily captures the noise. To improve accuracy, a Gaussian noise model is applied to the residual within the band regions. The final noise estimation is taken as the average of the residual. Using this estimation as a threshold, the algorithm computes the penalization by counting the number of Raman shifts where the baseline exceeds both the spectral intensity and the noise threshold distance. Given $\text{Penalized}_{\text{RS}}$ the number of Raman Shifts penalized and $\text{Total}_{\text{RS}} = |\{\tilde{\nu}_1,\tilde{\nu}_2,...,\tilde{\nu}_z\}|$ the total number of Raman Shifts, the comprehensive penalization is formalized in eq 24

$$\text{Intensity}_{\text{Penalization}} = \frac{\text{Penalized}_{\text{RS}}}{(\text{Total}_{\text{RS}} - \text{Penalized}_{\text{RS}})} \tag{24}$$

RESULTS

Validation of the Algorithm on Complex Biological Data

Overall, a good baseline should ideally follow the underlying Raman signal, ensuring that it does not alter any important peaks corresponding to chemical features, as these represent information about the molecular composition and structure of the sample. At the same time, baseline correction must effectively remove the background signals, such as fluorescence, which obscure the Raman signal. Any deviation from a

https://doi.org/10.1021/acsomega.5c09870
ACS Omega 2026, 11, 25057−25068

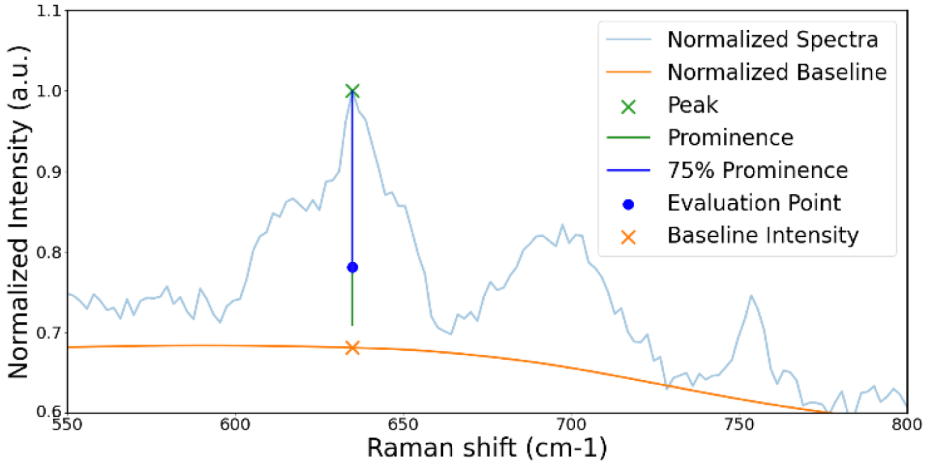


Figure 6. Single peak penalization and evaluation points used to detect overfitting.

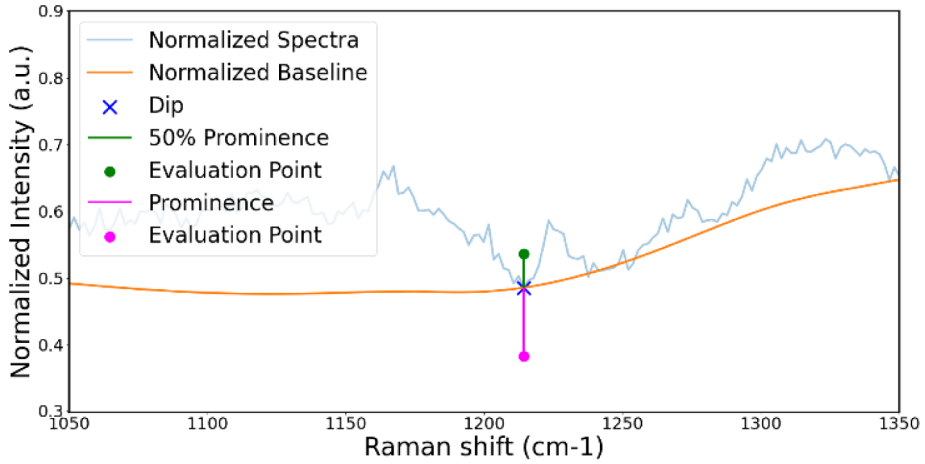


Figure 7. Single dip penalization and evaluation points used to detect underfitting.

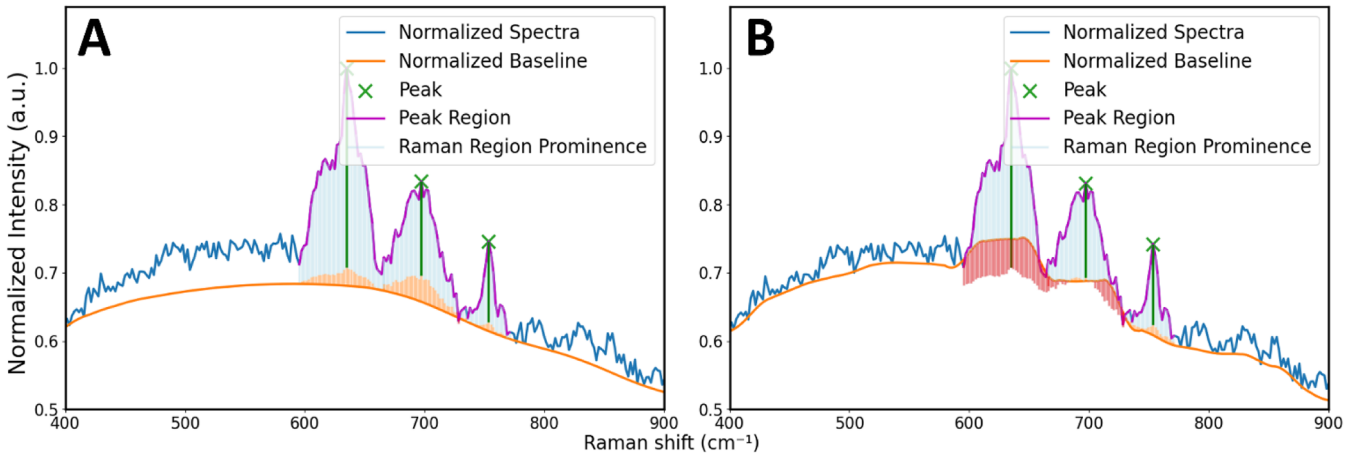


Figure 8. Example of peak region penalization for an underfitting (A) baseline with orange lines as the penalization and an overfitting (B) baseline correction algorithm with red lines as the penalization.

good baseline is penalized in the calculation of the IS-Score, as demonstrated below using a two-layer polymer−blood cell data set, where the Raman background is influenced by both the polymer and cell layers.[21] Figure 6 shows the evaluation point used to compute the single peak penalization. As stated previously, it is defined by subtracting 75% of the peak prominence from its intensity. In this case, the evaluation point helps assess baseline overfitting—if the baseline intensity at the peak position exceeds the intensity at the evaluation point, it indicates the baseline is following the signal too closely. Conversely, Figure 7 shows a dip with the first evaluation point—defined as half of the dip's prominence (green point)—and the second evaluation point corresponding to full dip prominence (magenta point). These two points help to

https://doi.org/10.1021/acsomega.5c09870
ACS Omega 2026, 11, 25057−25068

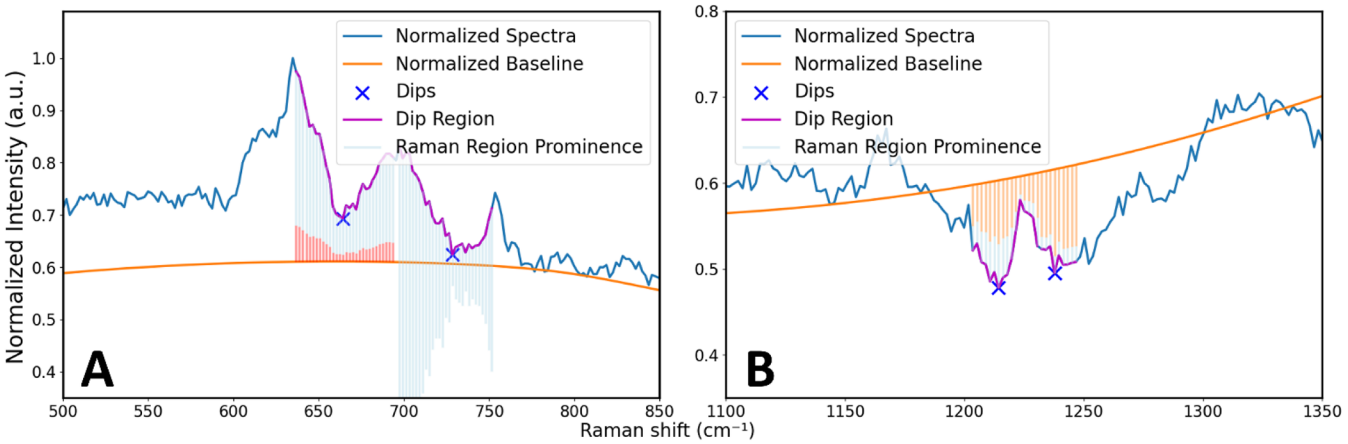


Figure 9. Example of dip region penalization for an underfitting baseline (A) with red lines as penalization and overfitting (B) with orange lines as penalization.

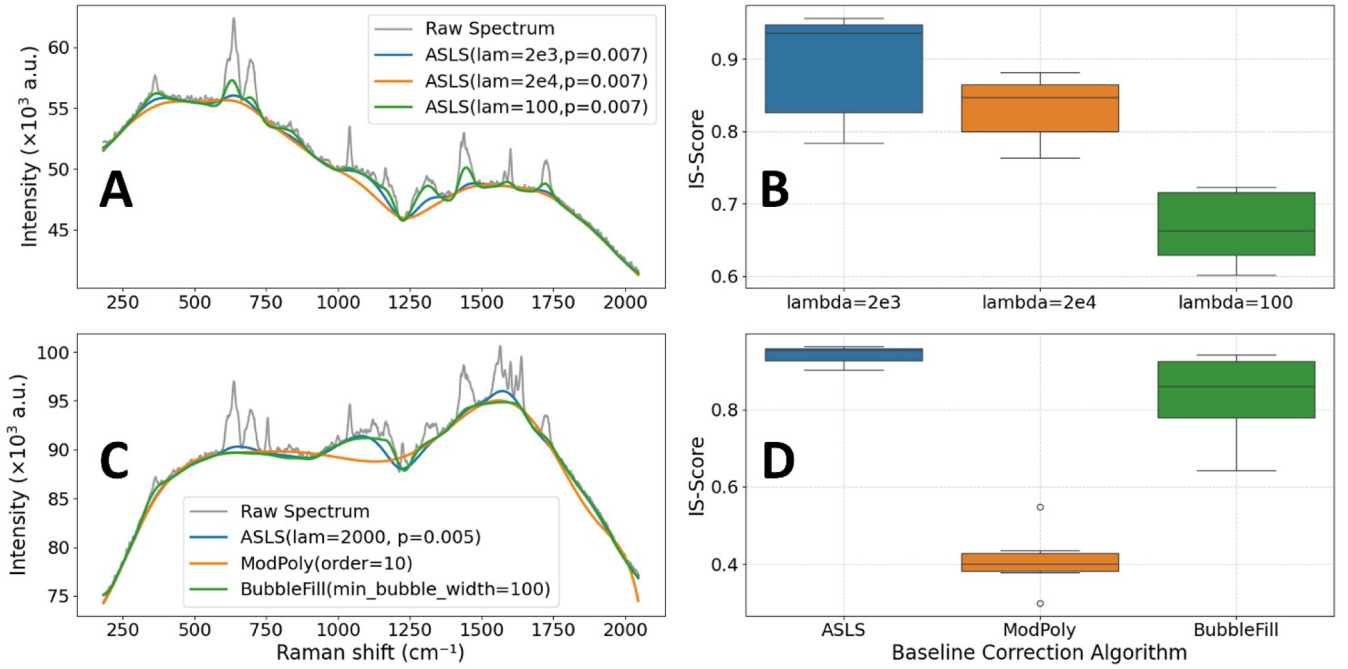


Figure 10. Results of the IS-Score for two different Raman spectroscopy data set. Plot (A) and (B) present the results for the polymer-only results, while panels (C) and (D) correspond to the blood-through-polymer data set. (A) and (C) show the mean spectra of the entire data set with the fitted baseline used, while (B) and (D) display a boxplot with the IS-Score for each baseline correction algorithm evaluated.

assess the underfitting scenario of a baseline. The peak region penalization strategy is illustrated in Figure 8 which highlights the penalized regions in orange and red across three peaks under two different baseline fitting scenarios. This approach can identify both overfitting and underfitting. Figure 8A shows a slightly underfitting scenario; each orange vertical line corresponds to the distance between the Raman Region Prominence and the baseline. Conversely, Figure 8B illustrates an overfitting case where the red lines represent the absolute distance between the Raman Region Prominence and the baseline. The same concept is applied to the dip region. Figure 9A and B illustrates this penalization in an underfitting and overfitting condition, respectively.

In Figure 9A, the baseline lies below the spectral dips, showing a clear underfitting pattern, with significant deviation from the true signal, while Figure 9B demonstrates a baseline exceeding the dip intensities, indicating a kind of overfitting and not a proper baseline fitting.

IS-Score Evaluation

To assess the effectiveness of the IS-Score, two experiments were conducted using two Raman spectroscopy data sets. In the first experiment, shown in Figure 10A and B, the same baseline correction algorithm Asymmetric Least Squares (ASLS) was applied to the first data set (only polymer spectra) using different parameter settings. Figure 10A shows the first data set average Raman spectrum along with the fitted baselines. Figure 10B displays the IS-Score boxplots for each parameter configuration plotted for 54 polymer spectra. The green baseline, corresponding to a λ value of 100, visibly removes important spectral features, including peaks at around 600 and 1400 cm^{-1}. As a result, it produces a lower IS-Score, indicating poor baseline fitting. In contrast, the blue baseline (λ

https://doi.org/10.1021/acsomega.5c09870
ACS Omega 2026, 11, 25057−25068

= 2e3) yields higher IS-Score values, averaging between 0.8 and 0.9, suggesting better performance. The orange baseline, corresponding to λ = 2e5, exhibits consistently low IS-Score values. To further test the robustness of the IS-Score, a second experiment was performed using a more complex polymer−blood data set and three different baseline correction algorithms (Figure 10C and D). Figure 10C presents the average Raman spectrum with the corresponding baselines fitted by each algorithm. Figure 10D presents the IS-Score boxplot for the three methods plotted for 54 spectra. ASLS achieved the highest scores, mostly ranging between 0.80 and 0.87, followed by BubbleFill. ModPoly performed the worst, with the lowest IS-Scores, and it removed the signal component around 700−900 cm^{-1}, visible in the average spectrum plot.

DISCUSSION

For the polymer data set, the results suggest that the green baseline (λ = 100) exhibits overfitting behavior, as it removes relevant spectral features such as peaks around 600 and 1400 cm^{-1} (Figure 10A). The IS-Score successfully penalizes this behavior by assigning lower scores. Conversely, the blue baseline (λ = 2e3) appears to balance trend-following and flexibility, achieving a better baseline correction, as indicated by higher IS-Score values. The orange baseline (λ = 2e5) reflects underfitting, failing to follow subtle spectral curvatures. Overall, these findings underscore the importance of careful parameter selection in baseline correction and highlight the IS-Score's utility in guiding this process. The results for the second data set indicate that the ModPoly algorithm tends to underfit the data, inadvertently removing meaningful spectral information, particularly in the 700−900 cm^{-1} region, while the ASLS achieved more accurate baseline correction with higher IS-Score values and better preserving relevant spectral features (Figure 10C). BubbleFill performed moderately well as the trend is similar to the ASLS; however, it is less consistent, as the peaks in the area of 650−700 cm^{-1} are not properly fitted. The significant spread in IS-Score values between the methods underscores the importance of quantitative evaluation in baseline correction. Even when baseline results may appear qualitatively similar, the IS-Score effectively highlights systematic differences, offering a robust basis for method selection in sensitive applications. Previous validation strategies such as RMSE rely on comparing fitted baselines against a known or simulated ground truth, which cannot fully capture the variability of experimental measurements and are hard to synthesize for complex biological data.[13−15] Computational learning-based strategies have also been explored for baseline correction. The genetic algorithm with the analytical marker offers automatic optimization but remains model- and task-dependent,[17] while deep learning approaches achieve simultaneous baseline correction and denoising with faster acquisition.[11,12] However, such methods rely heavily on large synthetic training data sets with ground-truth baselines and simulated error metrics, which can limit their applicability to real experimental data. Wavelength-shift Raman spectroscopy[23] has historically been used for fluorescence background correction by exploiting the fact that Raman bands shift predictably with small changes in excitation wavelength, whereas fluorescence remains static. Subtracting spectra from two wavelengths can, in theory, isolate and remove the fluorescence. However, in complex biological samples, this often introduces artifacts such as negative peaks or distorted Raman features, particularly when diagnostically relevant subtle differences are masked during reconstruction. Recently, a cross-wavelength correlation strategy[24] has been proposed, which evaluates baseline correction quality by measuring the consistency of Raman parameters (e.g., band positions, intensities) across multiple excitation wavelengths, providing a physically meaningful indication of wavelength-invariant molecular signatures. Despite this advantage, the need for multiwavelength acquisition complicates workflows, and resonance effects can alter spectral profiles independently of baseline quality, reducing robustness. As a result, such instrument-driven strategies are best suited to controlled settings, such as isolated molecules or pharmaceuticals, but are less practical for clinical or high-throughput studies, where single-wavelength protocols dominate. To the best of our knowledge, this is the first attempt to address this problem from an algorithm perspective, relying on only the raw spectrum and its baseline-corrected version. This enables the assessment of entire Raman spectroscopy data sets, helping to identify poorly fitted spectra and outliers. This streamlines the evaluation of multiple baseline correction algorithms simultaneously, simplifying the process of effective preprocessing in Raman spectroscopy. While the IS-Score metric provides a solid indication of fit quality, in the absence of a ground-truth baseline, the assessment retains some uncertainty and should be interpreted as indicative rather than absolute. Additionally, computing it for each spectrum increases the processing time. Nevertheless, the IS-Score versatility makes it a valuable tool for a wide range of Raman spectral analysis while also reducing the time required from experts. Additional results are provided in the Supporting Information where the IS-Score was tested in other domains such as food science (Figures S1, S2), pharmaceuticals (Figures S3, S4), and minerals (Figure S5). Furthermore, the full implementation, documentation, and a GUI are available on GitHub (Figures S6, S7) to enhance usability. We evaluated the computational cost of the algorithm on a system equipped with an Intel(R) Xeon(R) Gold 6240 CPU @ 2.60 GHz. To assess scalability, we generated 20 data sets with increasing sizes (500 to 10,000 spectra, in increments of 500), derived from the same raw Raman spectra, with augmented random noise and their asymmetric least-squares (ASLS) baseline-corrected versions. Despite involving multiple stages to compute the final metric, the runtime remained manageable for large data sets. For 500 spectra, the total execution time was 27 s. A data set of 5000 spectra required 4 min and 43 s, and the largest data set of 10000 spectra completed in 9 min and 15 s with runtime influenced primarily by the number of detected peaks and dips, and the length of the spectral axis. In this spectrum used for benchmarking, the algorithm identified 8 peaks and 9 dips across 814 Raman shifts.

CONCLUSION

Traditionally, the quality of a baseline correction method is evaluated through visual inspection of the Raman spectrum and its fitted baseline. While effective, this approach is time-consuming and impractical for large data sets, particularly with the increasing use of machine learning, which requires large high-quality preprocessed data sets. In this study, we proposed an algorithm called IS-Score that generated a numerical assessment that quantified the quality of the baseline fitting without requiring manual inspection of each Raman spectrum.

https://doi.org/10.1021/acsomega.5c09870
ACS Omega 2026, 11, 25057−25068

The subjective nature of Raman data processing makes the development of a generic algorithm complex. For this reason, IS-Score integrates both local and global parameters, such as intensities, bands, and AUC, rather than relying on ground truth values. This framework was validated using two data sets, including the challenging blood−polymer data set with noisy spectra, where the IS-Score robustly identified limitations of specific baseline correction algorithms (e.g., overfitting, artifact introduction). By providing an automated, objective assessment of baseline correction, the IS-Score streamlines preprocessing workflows, enhances reproducibility, and supports the optimization of spectral analysis in complex analytical scenarios. Additionally, this quantitative assessment of baseline quality could be leveraged to guide or optimize baseline retrieval algorithms. The IS-Score could serve as an objective function in machine learning frameworks, such as neural networks, enabling models to learn to predict optimal baselines directly from Raman spectra. Such a feedback loop could automatically adjust baseline parameters, or even baseline models to systematically maximize the IS-Score (i.e., spectral integrity), reducing manual intervention and ensuring consistency across large data sets. This approach opens a promising avenue for future development, where baseline correction is both automated and quantitatively optimized, enhancing the reliability and reproducibility of Raman spectral analysis in clinical and research applications.

■ ASSOCIATED CONTENT

Supporting Information

The Supporting Information is available free of charge at https://pubs.acs.org/doi/10.1021/acsomega.5c09870.

Additional experimental validation and screenshots of the Graphic User Interface; IS-Score and GUI implementation and documentation are available on GitHub: https://github.com/InnocenteSimone/IS_Score (PDF)

■ AUTHOR INFORMATION

Corresponding Authors

Simone Innocente − *Biophotonics@Tyndall, Tyndall National Institute, Cork T12 R5CP, Ireland; School of Computer Science and Information Technology, University College Cork, Cork T12 XF62, Ireland;* orcid.org/0009-0002-2237-513X; Email: simone.innocente@tyndall.ie

Rekha Gautam − *Biophotonics@Tyndall, Tyndall National Institute, Cork T12 R5CP, Ireland;* orcid.org/0000-0002-1176-8491; Email: rekha.gautam@tyndall.ie

Authors

Andrea Visentin − *School of Computer Science and Information Technology and Insight Centre for Data Analytics, University College Cork, Cork T12 XF62, Ireland*

Stefan Andersson-Engels − *Biophotonics@Tyndall, Tyndall National Institute, Cork T12 R5CP, Ireland; School of Physics, University College Cork, Cork T12 YN60, Ireland*

Katarzyna Komolibus − *Biophotonics@Tyndall, Tyndall National Institute, Cork T12 R5CP, Ireland*

Complete contact information is available at: https://pubs.acs.org/10.1021/acsomega.5c09870

Author Contributions

S.I. defined the project together with K.K., R.G., A.V., and S.I. designed and implemented the algorithm and conducted the analysis. K.K., R.G., A.V., and S.A.-E. contributed to supervising the study and reviewed the draft. All authors have approved the final version of the manuscript.

Notes

The authors declare no competing financial interest.

■ ACKNOWLEDGMENTS

This publication has emanated from research conducted with the financial support of Taighde´ Eireann−Research Ireland primarily (Grant No. 22/RP 2TF/10293) and secondarily by SFI (Grant No. 12/RC/2289-P2) cofounded under the European Regional Development Fund. For the purpose of Open Access, the author has applied a CC BY public copyright license to any author-accepted manuscript version arising from this submission. All the images used in the manuscript were created entirely by the authors; therefore, no external permission is required. Icons made by smashingstocks from Flaticon.com.

■ REFERENCES

(1) Lussier, F.; Thibault, V.; Charron, B.; Wallace, G. Q.; Masson, J.-F. Deep Learning and Artificial Intelligence Methods for Raman and Surface-Enhanced Raman Scattering. *TrAC Trends Anal. Chem.* **2020**, *124*, 115796.

(2) Gautam, R.; Vanga, S.; Ariese, F.; Umapathy, S. Review of Multidimensional Data Processing Approaches for Raman and Infrared Spectroscopy. *EPJ. Tech. Instrum.* **2015**, *2* (1), 8.

(3) Chen, H.; Xu, W.; Broderick, N. G. R. An Adaptive and Fully Automated Baseline Correction Method for Raman Spectroscopy Based on Morphological Operations and Mollification. *Appl. Spectrosc.* **2019**, *73* (3), 284−293.

(4) Lieber, C. A.; Mahadevan-Jansen, A. Automated Method for Subtraction of Fluorescence from Biological Raman Spectra. *Appl. Spectrosc.* **2003**, *57* (11), 1363−1367.

(5) Zhao, J.; Lui, H.; McLean, D. I.; Zeng, H. Automated Autofluorescence Background Subtraction Algorithm for Biomedical Raman Spectroscopy. *Appl. Spectrosc.* **2007**, *61* (11), 1225−1232.

(6) Baek, S.-J.; Park, A.; Ahn, Y.-J.; Choo, J. Baseline Correction Using Asymmetrically Reweighted Penalized Least Squares Smoothing. *Analyst* **2015**, *140* (1), 250−257.

(7) Li, J.; Choo-Smith, L.-P.; Tang, Z.; Sowa, M. G. Background Removal from Polarized Raman Spectra of Tooth Enamel Using the Wavelet Transform. *J. Raman Spectrosc.* **2011**, *42* (4), 580−585.

(8) Xi, Y.; Li, Y.; Duan, Z.; Lu, Y. A Novel Pre-Processing Algorithm Based on the Wavelet Transform for Raman Spectrum. *Appl. Spectrosc.* **2018**, *72* (12), 1752−1763.

(9) Chen, Y.; Dai, L. An Automated Baseline Correction Method Based on Iterative Morphological Operations. *Appl. Spectrosc.* **2018**, *72* (5), 731−739.

(10) Chen, T.; Son, Y.; Park, A.; Baek, S.-J. Baseline Correction Using a Deep-Learning Model Combining ResNet and UNet. *Analyst* **2022**, *147* (19), 4285−4292.

(11) Chen, T.; Son, Y.; Dong, C.; Baek, S.-J. Baseline Correction of Raman Spectral Data Using Triangular Deep Convolutional Networks. *Analyst* **2025**, *150* (12), 2653−2660.

(12) Sjöberg, J.; Siminea, N.; Păun, A.; Lita, A.; Larion, M.; Petre, I. RADAR: Raman Spectral Analysis Using Deep Learning for Artifact Removal. *Adv. Opt. Mate.r* **2025**, *13* (25), 2500736.

(13) He, S.; Zhang, W.; Liu, L.; Huang, Y.; He, J.; Xie, W.; Wu, P.; Du, C. Baseline Correction for Raman Spectra Using an Improved Asymmetric Least Squares Method. *Anal. Methods* **2014**, *6* (12), 4402−4407.

(14) Liu, J.; Sun, J.; Huang, X.; Li, G.; Liu, B. Goldindec: A Novel Algorithm for Raman Spectrum Baseline Correction. *Appl. Spectrosc.* **2015**, *69* (7), 834−842.
(15) Sheehy, G.; Picot, F.; Dallaire, F.; Ember, K.; Nguyen, T.; Petrecca, K.; Trudel, D.; Leblond, F. Open-sourced Raman spectroscopy data processing package implementing a baseline removal algorithm validated from multiple datasets acquired in human tissue and biofluids. *J. Biomed. Opt.* **2023**, *28* (2), 025002.
(16) Ou, Z.; Liu, J.; Meng, F. Evaluating Baseline Correction in Raman Spectroscopy: A Novel Cross-Wavelength Correlation Approach for Low-Maturity Organic Matter. *J. Raman Spectrosc.* **2025**, *56* (8), 733−740.
(17) Guo, S.; Bocklitz, T.; Popp, J. Optimization of Raman-Spectrum Baseline Correction in Biological Application. *Analyst* **2016**, *141* (8), 2396−2404.
(18) Das, R. S.; Agrawal, Y. K. Raman Spectroscopy: Recent Advancements, Techniques and Applications. *Vib. Spectrosc.* **2011**, *57* (2), 163−176.
(19) Cutshaw, G.; Uthaman, S.; Hassan, N.; Kothadiya, S.; Wen, X.; Bardhan, R. The Emerging Role of Raman Spectroscopy as an Omics Approach for Metabolic Profiling and Biomarker Detection toward Precision Medicine. *Chem. Rev.* **2023**, *123* (13), 8297−8346.
(20) Lemes, E. M. Raman Spectroscopy − a Visit to the Literature on Plant, Food, and Agricultural Studies. *J. Sci. Food Agric.* **2025**, *105* (4), 2128−2133.
(21) Gautam, R.; Oh, J.-Y.; Patel, R. P.; Dluhy, R. A. Non-Invasive Analysis of Stored Red Blood Cells Using Diffuse Resonance Raman Spectroscopy. *Analyst* **2018**, *143* (24), 5950−5958.
(22) Taskesen, E. *Findpeaks is for the detection of peaks and valleys in a 1D vector and 2D array (image). (Version 2.3.1)*; Zenodo, 2020. https://erdogant.github.io/findpeaks.
(23) Virtanen, P.; Gommers, R.; Oliphant, T. E.; Haberland, M.; Reddy, T.; Cournapeau, D.; Burovski, E.; Peterson, P.; Weckesser, W.; Bright, J.; et al. SciPy 1.0: Fundamental Algorithms for Scientific Computing in Python. *Nat. Methods* **2020**, *17* (3), 261−272.
(24) Gebrekidan, M. T.; Knipfer, C.; Stelzle, F.; Popp, J.; Will, S.; Braeuer, A. A Shifted-Excitation Raman Difference Spectroscopy (SERDS) Evaluation Strategy for the Efficient Isolation of Raman Spectra from Extreme Fluorescence Interference. *J. Raman Spectrosc.* **2016**, *47* (2), 198−209.



https://doi.org/10.1021/acsomega.5c09870
ACS Omega 2026, 11, 25057−25068